Endoplasmic reticulum (ER) stress and cAMP/PKA pathway mediated Zn-induced hepatic lipolysis

Yu–Feng Song [a], Christer Hogstrand [b], Chuan-Chuan Wei [a], Kun Wu [a], Ya–Xiong Pan[a], Zhi Luo [a, c,*]

[a] *Key Laboratory of Freshwater Animal Breeding, Ministry of Agriculture, Fishery College, Huazhong Agricultural University, Wuhan 430070, China*

[b]*Diabetes and Nutritional Sciences Division, School of Medicine, King's College London, Franklin-Wilkins Building, 150 Stamford Street, London, SE1 9NH, UK*

[c] *Collaborative Innovation Center for Efficient and Health Production of Fisheries in Hunan Province, Changde 415000, China*

Corresponding author. Prof. Zhi Luo, Tel.: +86-27-8728-2113; Fax: +86-27-8728-2114; Email address: luozhi99@mail.hzau.edu.cn; luozhi99@aliyun.com (Z. Luo).

Abstract

The present study was performed to determine the effect of Zn exposure influencing endoplasmic reticulum (ER) stress, explore the underlying molecular mechanism of Zn-induced hepatic lipolysis in a fish species of significance for aquaculture, yellow catfish *Pelteobagrus fulvidraco*. We found that waterborne Zn exposure evoked ER stress and unfolded protein response (UPR), and activated cAMP/PKA pathway, and up-regulated hepatic lipolysis. The increase in ER stress and lipolysis were associated with activation of cAMP/PKA signaling pathway. Zn also induced an increase in intracellular Ca^{2+} level, which could be partially prevented by dantrolene (RyR receptor inhibitor) and 2-APB (IP3 receptor inhibitor) , demonstrating that the disturbed Ca^{2+} homeostasis in ER contributed to ER stress and dysregulation of lipolysis. Inhibition of ER stress by PBA attenuated UPR, inhibited the activation of cAMP/PKA pathway and resulted in down-regulation of lipolysis. Inhibition of protein kinase RNA-activated-like ER kinase (PERK) by GSK2656157 and inositol-requiring enzyme (IRE) by STF-083010 differentially influenced Zn-induced changes of lipolytic metabolism, indicating that PERK and IRE pathways played different regulatory roles in Zn-induced lipolysis. Inhibition of PKA by H89 blocked the Zn-induced activation of cAMP/PKA pathway with a concomitant inhibition of ER stress-mediated lipolysis. Taken together, our findings highlight the importance of the ER stress–cAMP/PKA axis in Zn-induced lipolysis, which provides new insights into Zn toxicology in fish and probably in other vertebrates.

Capsule abstract

Zn exposure evoked ER stress and dysregulation of Ca^{2+} homeostasis, and then activated cAMP/PKA pathway and resulted in hepatic lipolysis.

Graphical abstracts

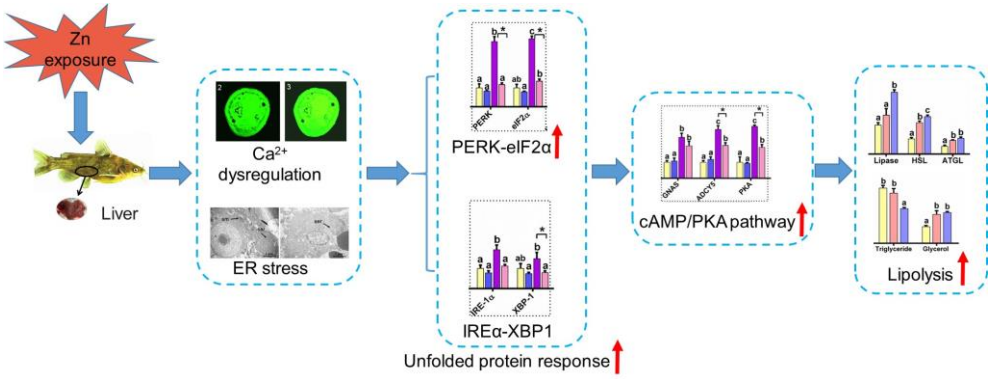

Highlights

- ER stress contributed to Zn-evoked lipolysis.
- Dysregulation of lipolytic process was partially attributable to the release of Ca^{2+} from the ER.
- PERK–eIF2α and IRE1α–XBP1 pathways played different roles in Zn-induced lipolysis.
- cAMP/PKA pathway mediated Zn-induced lipolysis after ER stress.

Keywords: Zn; Lipid metabolism; Endoplasmic reticulum stress; Unfolded protein response; cAMP/PKA pathway

1. Introduction

The endoplasmic reticulum (ER) is a multifunctional intracellular organelle that controls protein quality and is responsible for xenobiotic detoxification and Ca^{2+} homeostasis (Biwer & Isakson, 2016). Disruption in ER homeostasis creates a state defined as ER stress, and initiates a complex signaling network called as the unfolded protein response (UPR) (Volmer & Ron, 2015). Many environmental and physiological insults can disturb ER homeostasis and activate UPR

(Han and Kaufman, 2016). UPR is an integrated intracellular signaling pathway that induces translational inhibition followed by upregulation of ER-resident chaperones, such as GRP78/BiP, GRP94, and CRT **(**Volmer & Ron, 2015). In addition, the UPR is mediated by three pathways, the PERK-eIF2α pathway, the IRE1α-XBP1 pathway, and the activating transcription factor 6 (ATF6) pathway (Wang & Kaufman, 2012). Each pathway has different signaling components and culminates in transcriptional regulation of different gene expression during ER stress (Bozaykut et al., 2016; Wang & Kaufman, 2012). On the other hand, as the most important intracellular calcium store, the ER plays a key role in intracellular calcium homeostasis (Biwer & Isakson, 2016). Ca^{2+} release from ER stores is mediated via the inositol 1,4,5-triphosphate (InsP3) receptor (Ferreiro et al., 2004) and the ryanodine receptor (RyR) (Taylor & Laude, 2002). Disturbance of intracellular Ca^{2+} homeostasis triggers the ER stress response (Michalak et al., 2002). Moreover, the lumenal and/or cytoplasmic side of ER membrane is the site of triglyceride (TG) synthesis and nascent lipid droplet formation. Several evidences indicated that ER stress and UPR regulated hepatic lipid metabolism via lipogenesis at transcriptional levels in mammals (Basseri & Austin, 2011; Zhang et al., 2012). In fish, our recent studies also suggested that ER stress and UPR could control hepatic lipogenic metabolism by activating SREBP-1c (Song et al., 2016a,b).

TG is an essential source of energy for many tissues, and TG lipolysis produces glycerol and free fatty acids (FFA) (Londos et al., 1999). The regulation of lipolysis is complex, and many enzymes and signaling pathways take part in the hydrolysis of TG. These lipolytic enzymes included hepatic lipase (HL), adipose triglyceride lipase (ATGL), hormone-sensitive lipase (HSL) and monoacylglycerol lipase (MGL) (Fredrikson et al., 1986; Kim et al., 2016). One of the predominant signaling pathway that activates lipolysis is the cyclic AMP (cAMP) dependent

pathway. Lipolytic stimuli increases lipolysis by activating adenylyl cyclase (ADCY) and raising intracellular levels of cAMP, with resultant activation of cAMP-dependent protein kinase (PKA) (Larsson et al., 2016). Studies also suggested that ER stress could increase lipolysis through activation of the cAMP/PKA pathway (Deng et al., 2012). At present, although the role and mechanism of ER stress and UPR in hepatic lipogenesis have been explored in mammals (Basseri & Austin, 2011; Gentile et al., 2011), the mechanisms of ER stress accelerating lipolysis remained unknown (Brasaemle & Wolins, 2012). In fish, to our best knowledge, no studies are conducted to elucidate the potential role of the ER stress and UPR in the modulation of the lipolysis.

Zinc (Zn) is an essential micronutrient required for numerous important biological functions, including enzymatic activity, protein structure and signaling (Hogstrand, 2012). However, when present in excess amounts, it can exert adverse effects (Zheng et al., 2013). In humans, Zn supplementation affects lipid metabolism (Ranasinghe et al., 2015). Our recent studies indicated that waterborne Zn exposure can induce lipid accumulation through improvement of lipogenesis in yellow catfish *Pelteobagrus fulvidraco*, an omnivorous freshwater fish (Zheng et al., 2013). In contrast, in javelin goby *Synechogobius hasta*, a carnivorous fish species, waterborne Zn exposure decreased hepatic lipid deposition (Huang et al., 2016). Moreover, even in the same fish species, differential effects on hepatic lipid deposition and metabolism were found between chronic and acute Zn exposure, and also between waterborne and dietborne Zn exposure (Zheng et al., 2013; 2015). Thus, it seems that effect of Zn on lipid deposition and metabolism might be complex, and many mechanisms may be involved in the process. Accordingly, it is important to investigate the effects and mechanism of Zn exposure on lipolysis in fish. To this end, in the present study, the effect and mechanism of Zn-induced lipolysis were investigated, and the

potential roles of ER stress, dysregulation of Ca^{2+} homeostasis and cAMP/PKA pathway in this processes was also determined. The results will be beneficial to elucidate the importance of the ER stress–cAMP/PKA axis in Zn-induced lipolysis, which provides new insights into Zn toxicology in fish and probably in other vertebrates.

2. Materials and methods

2.1. Drug treatment

The stock solution of $ZnSO_4 \cdot 7H_2O$ was prepared to a concentration of 1 M with sterile double-distilled water. 2-APB, dantrolene, PBA, GSK2656157, STF-083010 and H89 were dissolved in DMSO. All the inhibitors used in our trial were selected according to other studies: 2-APB (inhibitors of the ER Ca^{2+}-release channels IP3 receptors, Gerasimenko et al., 2010), dantrolene (inhibitors of the ER Ca^{2+}-release channels RyR receptors, Ferreiro et al., 2004), PBA (inhibitor of ER stress, Erbay et al., 2009; Song et al., 2016b), GSK2656157 (inhibitor against the PERK pathway, Atkins et al., 2013; Axten et al., 2013), STF-083010 (inhibitor against the IRE pathway, Tufanli et al., 2017; Tang et al., 2014) and H 89 (inhibitor against PKA pathway, Chijiwa et al., 1990). The concentrations of 2-APB (50 μM), dantrolene (30 μM), PBA (100 μM), GSK2656157 (10 μM), STF-083010 (50 μM) and H 89 (30 μM) were selected according to our pilot experiment in yellow catfish (Song et al., 2016b) and studies in mammals (Atkins et al., 2013). The maximal DMSO concentration had no discernible effect on cell viability and other biological parameters. The Zn concentrations (30 μM) in the *in vitro* experiment were used based on IC50 of Zn obtained from our earlier studies (unpublished data).

2.2. Experimental treatments

Four experiments were performed. We assured that the experiments followed the guidelines

of Institutional Animal Care and Use Committee (IACUC) of Huazhong Agricultural University, Wuhan of China.

2.2.1 Exp. 1: investigating effects of waterborne Zn exposure on hepatic lipolysis and ER stress in vivo

Yellow catfish maintenance and Zn exposure were carried out in semi-static aquarium system according to our published protocol (Song et al., 2016b; Zheng et al., 2013). Briefly, 216 uniform-sized fish (mean weight: 8.54 ± 0.36 g, mean ± SEM) were stocked in 9 fiberglass tanks (300-l in water volume), 24 fish per tank. They were exposed three different Zn concentrations, three replicates for each Zn concentration (zero, 0.25 , and 0.5 mg Zn/l, corresponding to 0, 2.5 and 5% of the 96 h LC50 of Zn for *P. fulvidraco*, Zheng et al., 2013). The fish were fed twice daily with commercial diets (Zn content is 17.45 mg/kg diet). During the experiment, measured waterborne Zn concentrations from three treatments were 0.007 ± 0.001, 0.253 ± 0.004, and 0.514 ± 0.070 mg Zn/l, respectively. The experiment continued for 56 days and sampling occurred on day 28 and day 56, respectively.

2.3.2. Exp. 2: investigating the involvement of the Ca^{2+} release from ER in Zn-induced ER stress in vitro

Hepatocytes were isolated from *P. fulvidraco* liver according to our recent studies (Zhuo et al., 2014; Song et al., 2015). Ca^{2+} measurement was performed according to the methods described in our studies (Song et al., 2016a,b). Hepatocytes were stained with 5 μM Fluo-4/AM in HBSS for 30 min at 28 °C after pretreated with 2-APB, or dantrolene for 2 h.

2.3.3. Exp. 3: Exploring the potential role and mechanism of ER stress and UPR in Zn-induced lipolysis in vitro

The primary hepatocytes were plated into 25 cm^2 flasks at a concentration of 2×10^5 cells/ml and incubated with M199 medium containing 1 mmol/l L-glutamine, 5% (v/v) FBS, penicillin (100 IU/ml) and streptomycin (100 μg/ ml), at 28 °C in the humidified air containing 5% CO_2. For signaling pathway verification experiment, eight groups were designed: control (containing 0.1% DMSO), PBA (100 μM), GSK2656157 (10 μM), STF-083010 (50 μM), Zn (30 μM), PBA (100 μM) + Zn (30 μM), GSK2656157 (10 μM) + Zn (30 μM), STF-083010 (50 μM) + Zn (30 μM), respectively. Each treatment was conducted in triplicate. The inhibitors (PBA, GSK2656157 and STF-083010) were added 2 h prior to the addition of Zn. The cells were gathered for the following analysis after 18 h.

2.3.4. Exp. 4: investigating the potential role of cAMP/PKA pathway in Zn-induced lipolysis

For the H89 treatment experiment, four groups were designed as follows: control (containing 0.1% DMSO), H89 (30 μM), Zn (30 μM), H89 (30 μM) + Zn (30 μM), respectively. Each treatment was performed in triplicate. H89 was added 2 h prior to the addition of Zn. The cells were gathered for the following analysis after 18 h.

2.3. Sample analysis

2.3.1. Ultrastructural observation and determination of Zn, TG and glycerol contents, and lipase activity

Ultrastructural analyses were performed according to our recent studies (Song et al., 2013; 2014). Zn content was assayed with the inductively coupled plasma atomic emission spectrometry (ICP-AES) (Song et al., 2014). TG and glycerol were determined following the method of Song et al. (2015). Analysis of lipase activity followed the method described in Ren et al. (2011).

2.3.2. Assay of cAMP and PKA levels, and HSL and ATGL activities

cAMP and PKA levels was performed according to the methods described previously (Newton et al., 2011), using the direct cAMP and PKA ELISA kit (Enzo Life Sciences). This assay of HSL was performed according to Frayn et al. (1993) and Reynisdottir et al. (1997). ATGL activity followed the method of Basu et al. (2011).

2.3.3. Confocal fluorescence microscopic $[Ca^{2+}]_i$ measurement

The Ca^{2+} imaging acquisition was performed as described in Gazarini et al. (2003) and our studies (Song et al., 2016a, b). Experiments were performed with at least three different cell preparations, and 15–20 cells were monitored in each experiment.

2.3.4. mRNA level determination by real-time Q-PCR

Analyses on gene transcript levels were conducted by quantitative real-time PCR (RT-qPCR) method described in our studies (Zheng et al., 2013; Song et al., 2016a, b). The primer sequences used in this analysis are given in Supplementary Table 1. A set of eight housekeeping genes (β-actin, GAPDH, EF1A, 18S rRNA, HPRT, B2M, TUBA and RPL17) were selected from our transcriptome database in order to test their transcription stability. Our pilot experiment indicated that β-actin and TUBA (β-actin and TUBA, M=0.25) showed the most stable level of expression across the experimental conditions as suggested by geNorm (Vandesompele et al., 2002). Thus, the relative expression levels were normalized to the geometric mean of the combination of two genes and calculated using the $2^{-\Delta\Delta Ct}$ method (Livak & Schmittgen, 2001).

2.4. Statistical analysis

All data were expressed as mean ± standard error of means (SEM). The normality of data

196 distribution and the homogeneity of variances were analyzed by the Kolmogorov–Smirnov test
197 and Bartlett's test, respectively. Then, data were subjected to one-way ANOVA and Tukey's
198 multiple range test using SPSS 17.0 software. $P < 0.05$ was considered significant. Differences
199 between day 28 and day 56 for the same Zn concentrations *in vivo*, and between inhibitors
200 groups and Zn groups *in vitro* were analyzed by Student's T-test for independent samples.

201 **3. Results**

202 *3.1. Chronic Zn exposure evokes ER stress and UPR, and activates lipolysis in vivo*

203 Waterborne Zn exposure resulted in a dose-dependent increase in liver Zn concentration,
204 but there were no effects on WG, SGR, survival, CF or VSI (Supplementary Table 2).

205 To study if Zn evoked ER stress and UPR, we first examined hepatic ultrastructural
206 alteration in *P. fulvidraco* following Zn exposure. Chronic Zn exposure caused the ER swelling,
207 which increased with waterborne Zn levels and with increasing exposure time (Fig. 1A). The
208 mRNA levels of ER stress marker genes (GRP78/BiP, GRP94 and CRT) were significantly
209 up-regulated in the Zn-exposed group, indicating the activation of ER stress (Fig. 1B and C). Zn
210 exposure also significantly up-regulated mRNA levels of hepatic PERK, eIF2α, IRE-1α and
211 XBP-1, but not ATF-6 mRNA level. The expression of genes involved in ER stress and UPR
212 were higher on day 56 than those on day 28.

213 In the present study, Zn exposure significantly up-regulated mRNA levels of the tested
214 genes, except for HSL1 and MGL on day 28 and for HSL1 on day 56 (Fig. 2A and B). At the
215 protein levels, cAMP and PKA tended to increase with increasing Zn concentration although the
216 difference in PKA level was not statistically significant on day 28 (Fig. 2C). At the enzyme
217 levels, lipase activities on both day 28 and day 56, and HSL and ATGL activities on day 56

increased with increasing Zn levels (Fig. 2D).

3.2. The Zn-induced increases in intracellular Ca^{2+} concentration were attributable to the release of Ca^{2+} from the ER

Compared to the control, Zn addition in the incubation medium markedly increased the intracellular Ca^{2+} concentration (Fig. 3A). Compared to single Zn incubation, 2-APB, the inhibitor of IP3 receptor, reduced the [Ca^{2+}] to about 75% (Fig. 3B). Dantrolene, which inhibits RyR, reduced the intracellular Ca^{2+} concentration to about 60% (Fig. 3C, D).

3.3. Two distinct UPR pathways (PERK–eIF2α and IRE1α–XBP1) show differential effects on Zn-induced lipolysis in vitro

The chemical ER chaperone, 4-phenylbutyrate (PBA) was used to confirm the potential role of ER stress and UPR in Zn-induced lipolysis. PBA markedly attenuated the Zn-induced up-regulation of gene expression involved in ER stress, UPR (GRP78/BiP, GRP94, CRT, PERK and eIF2α), and lipolysis (ADCY5, PKA, HSL2 and MGL) (Fig. S1A and B). At the same time, PBA also significantly attenuated the Zn-evoked elevation of cAMP and PKA levels, lipase and HSL activities, and glycerol contents (Supplementary Fig. 1C, D and E). Compared to single Zn group, Zn and PBA co-incubation significantly increased TG contents (Supplementary Fig. 1E).

GSK2656157 markedly alleviated the Zn-induced elevation of mRNA expression of GRP78/BiP, PERK, eIF2α, ADCY5, PKA and MGL (Fig. S2A and B). GSK2656157 also significantly attenuated the Zn-induced increase of cAMP and PKA levels, activities of lipase and ATGL, and glycerol contents, indicating the PERK–eIF2α involved Zn-induced lipolysis (Fig. S2C, D and E). STF-083010 significantly attenuated the Zn-induced elevation of mRNA expression of GRP78/BiP, GRP94, CRT, IRE1α, XBP1, HSL1, HSL2 and ATGL (Fig. 4A and

B). However, unlike GSK2656157, STF-083010 did not significantly influence the Zn-induced up-regulation of cAMP and PKA levels, and activities of lipase, HSL and ATGL, and TG and glycerol contents (Fig. 4C, D and E). Interestingly, compared with the Zn + STF-083010 group, the Zn + GSK2656157 group significantly down-regulated cAMP level, and lipase, HSL and ATGL activities, and glycerol content (Fig. 4C, D and E).

3.3. The activation of cAMP/PKA signaling pathway is involved in Zn-induced hepatic lipolysis in vitro

To determine the involvement of cAMP/PKA pathway activation in Zn-induced lipolysis, primary hepatocytes from *P. fulvidraco* were pretreated with H 89 (an inhibitor against the PKA pathway) and then with Zn exposure. Compared to the Zn alone treatment, pretreatment of H 89 markedly attenuated the Zn-induced increase of mRNA expression of GRP78/BiP, ADCY5, PKA, HSL1, HSL2, ATGL and MGL (Fig. 5A and B). Furthermore, H 89 also significantly attenuated the Zn-induced elevation of cAMP and PKA levels, and lipase, HSL and ATGL activities, and glycerol contents (Fig. 5C, D and E).

4. Discussion

Lipid metabolism is sensitive to changes in Znstatus in fish as well as in humans (Ranashinghe et al., 2015; Zheng et al., 2010, 2013). The present study, for the first time, explored the mechanism into Zn -induced lipolysis and provided evidence that ER stress and UPR mediated the Zn-induced hepatic lipolysis via cAMP/PKA pathway. Furthermore, using the inhibitors of UPR pathways, we also revealed the differential mechanisms of two UPR pathways (PERK–eIF2α and IRE1α–XBP1) on Zn-induced lipolysis in fish.

Our study indicated that waterborne Zn exposure activated ER stress and the UPR signaling pathway in liver of yellow catfish. First, Zn exposure significantly up-regulated hepatic mRNA expression of GRP78/BiP, GRP94 and CRT, in yellow catfish. Second, two UPR pathways, the PERK–eIF2α pathway and the IRE1α–XBP1 pathway were activated by Zn exposure. A similar activation of ER stress and UPR were also been found in *P. fulvidraco* exposed to Cu (Song et al., 2016b). Liu et al. (2006) also indicated that $CdCl_2$ exposure elevated the mRNA levels of Grp78 and eIF2α in LLC-PK1 cells. Qian & Tiffany-Castiglioni (2003) found that Grp78, IRE1 and ATF6 mRNA levels were upregulated by Pb exposure in the mammalian nerve cell, and IRE1/ATF6 and/or IRE1/JNK are the potential pathways during the process. Furthermore, Chen et al. (2015) demonstrated that Cd toxicity induced dramatic ER stress and may inhibit protein kinase B (AKT)/mTOR (mammalian target of rapamycin) pathway, which also play a central role in regulating lipolysis (Lamming et al., 2013). UPR pathways were activated to reduce the ER load of unfolded proteins under ER stress (Ron & Walter, 2007), which will in turn influence lipid metabolism (Oyadomari et al., 2008; Lee & Glimcher, 2009; Song et al., 2016a, b). We found that the expression of genes involved in ER stress in *P. fulvidraco* was higher on day 56 than on day 28, meaning the time-dependent effect on ER stress. Similar pattern was also observed in liver of *P. fulvidraco* following Cu exposure (Song et al., 2016b).

ER chaperones require high concentration of Ca^{2+} for their activities. Accordingly, strong modification in Ca^{2+} homeostasis can lead to ER stress (Xu et al., 2005). Here, the intracellular Ca^{2+} concentration significantly increased after Zn exposure. Similar observation was also obtained in McNulty & Taylor (1999) and Song et al. (2016b). Moreover, dantrolene or 2-APB significantly attenuated the intracellular Ca^{2+} elevation induced by Zn, suggesting the increase of intracellular Ca^{2+} level induced by Zn were attributable to the release of Ca^{2+} from the ER. Thus,

285 our present study indicated that Zn-evoked ER stress, at least in part, via Ca^{2+} release from ER.

286 One of objectives of the current study was to explore the mechanism of waterborne Zn
287 exposure inducing lipolysis. To this end, some lipolytic enzymes were determined. ATGL
288 catalyzes the initial step of lipolysis, converting TGs to diacylglycerols (DGs); HSL is mainly
289 responsible for the hydrolysis of DGs to monoacylglycerols (MGs) and MG lipase (MGL)
290 hydrolyzes MGs (Zechner et al., 2012). Our current study found the activities and/or expression
291 level of these enzymes were significantly up-regulated in liver of *P. fulvidraco* exposed to Zn,
292 indicating the activation of lipolysis. To our best knowledge, at present, little information is
293 available about the role of Zn in lipolysis, which made comparison rather difficult. In our earlier
294 studies, Zheng et al. (2015) found waterborne Zn exposures significantly upregulated ATGL
295 mRNA levels in muscle of *P. fulvidraco*, which implied the potential role of Zn in lipolysis in
296 fish. Fatty acids generated by lipolysis within the ER bilayer can serve as ligands for PPARα
297 activation and as substrates for mitochondrial ß-oxidation (Erickson et al., 2013). Moreover, the
298 current study also indicated the involvement of ER stress in Zn-induced activation of lipolysis in
299 *P. fulvidraco* since PBA, the inhibitor of ER stress, markedly attenuated the Zn-induced
300 up-regulation of gene expression involved in lipolysis (ADCY5, PKA, HSL2 and MGL), and
301 lipase and HSL activities. Similarly, Deng et al. (2012) found ER stress involved lipolysis
302 through up-regulation of GRP78 and activation of phosphorylation status of PERK and eIF2α in
303 rat adipocytes. In the current study, 4-PBA markedly attenuated the Zn-induced up-regulation of
304 GRP78/Bip and GRP94, and PERK and eIF2α, in agreement with our recent study on the effect
305 of 4-PBA on Cu-induced activation of ER stress in *P. fulvidraco* (Song et al., 2016b). Taken
306 together, these results suggest that ER stress and the UPR pathway were involved the activation
307 of Zn-induced lipolysis.

The mechanisms into activation of lipolysis by ER stress may be multifactorial. Studies suggested that cAMP and PKA are the major signals which regulate lipolysis (Londos et al., 1999). Deng et al. (2012) pointed out that the lipolytic effect of ER stress occurred with elevated cAMP production and PKA activity, and inhibition of PKA attenuated the lipolysis. This mechanism implicates the coupling of hormone receptors in the plasma membrane to a Gs family of GTP-binding proteins. The guanine nucleotide-binding protein G(s) subunit alpha (GANS) stimulates an ADCY, which produces cAMP. The resulting increase in intracellular cAMP levels leads to the activation of PKA (Larsson et al., 2016). PKA further influences the key enzyme that catalyzes TG and diglycerides breakdown, producing the subsequent release of FFA and glycerol. Intracellular TG undergoes lipolysis via the action of three major lipases: ATGL, HSL and monoacylglycerol lipase (MGL). cAMP reduced the levels of HSL mRNA expression and lipase activity via independent mechanisms, suggesting that sustained activation of PKA pathways exerts a negative control on HSL mRNA expression (Plee-Gautier et al., 1996). In the present study, Zn exposure increased the levels of cAMP and PKA, indicating the activation of cAMP/PKA signaling pathway. Intracellular cyclic AMP increase activates lipolysis while inhibition of lipolysis is associated with the reduction of cAMP levels (Lafontan & Langin, 2009). Accompanying these changes, total activity of cellular lipases was promoted to confer the lipolysis (Deng et al., 2012). Waterborne Zn exposure up-regulated mRNA expression of GANS, ADCY and PKA, which further supported the notion. Since Zn exposure activated cAMP/PKA signaling pathway in liver of *P. fulvidraco*, we next examined whether cAMP/PKA signaling pathway played a role in Zn-induced lipolysis. The involvement of PKA was further evidenced by the inhibitor H89, which suppressed the Zn induced increase in lipolysis. In the current study, H89, inhibitor of cAMP/PKA pathway, significantly blocked the Zn-induced lipolysis,

suggesting that cAMP/PKA activation was upstream of ER stress which mediated Zn-induced lipolysis. Similarly, Deng et al. (2012) suggested that the activation of cAMP/PKA is a major signaling event triggering the lipolytic cascade, and PKA inhibition by H89 inhibited the lipolysis. This protective effect was attenuated on PKA inhibition, which implicated an involvement of cAMP/PKA signals in modulating the UPR during ER stress, as suggested by Yusta et al. (2006) and Cunha et al. (2009). Therefore, these findings suggest that cAMP/PKA activation was involved Zn-induced lipolysis metabolism in *P. fulvidraco*.

Having determined the role of ER stress in Zn-induced lipolysis, we next explored the mechanisms underlying UPR pathways mediating Zn-induced lipolysis. Our current study demonstrated that GSK2656157 significantly blocked the Zn-induced activation of PERK–eIF2α pathway, in partial agreement with other studies (Gu et al., 2015; Jia et al., 2015). Most importantly, the present study indicated that blocking of PERK–eIF2α signaling was sufficient to inhibit the activation of cAMP/PKA pathway and to attenuate Zn-induced lipolysis. Similarly, Oyadomari et al. (2008) found that activation of the PERK pathway regulated lipid metabolism in the liver of mice. However, contrary to the PERK–eIF2α pathway, STF-083010 showed no markedly inhibitory effect on Zn-induced activation of cAMP/PKA pathway and lipolysis at enzymatic levels, and on contents of TG and glycerol in primary hepatocytes of *P. fulvidraco*. These findings implied that PERK–eIF2α and the IRE1α–XBP1 pathways played different roles in Zn-induced lipolysis. Similarly, Lakshmanan et al. (2013) suggested that the activation of PERK pathway are the major determinant for the ER stress-mediated metabolic dysfunction, rather than the IRE-1α-XBP1 pathway. Other studies indicated the differential effects and mechanisms of three UPR branches on regulating cell function and metabolism (Bobrovnikova-Marjon et al., 2008; Miyake et al., 2016). Indeed, the significant different effects

of GSK2656157 and STF-083010 on Zn-induced activation of cAMP/PKA pathway and lipolysis at enzymatic levels were also found in our present study, further supporting the above-mentioned notion.

5. Conclusions

Our study clearly indicated that Zn exposure evoked ER stress and disturbed Ca^{2+} homeostasis. cAMP/PKA pathway mediated Zn-induced ER stress which in turn led lipolysis. Two UPR pathways (PERK–eIF2α and IRE1α–XBP1 pathway) played different roles in regulating Zn-induced lipolysis. These findings highlight the importance of the ER stress–cAMP/PKA axis in the regulation of lipolysis under Zn exposure, and provide new insights into Zn toxicology in fish and probably in other vertebrates.

Conflict Of Interest

The authors declare that they have no conflicts of interest with the contents of this article.

Acknowledgments

This work was supported by the National Natural Science Foundation of China (grant no. 31422056), the Fundamental Research Funds for the Central Universities, China (grant nos. 2662015PY017, 2014JQ002), and by China Postdoctoral Science Foundation (grant nos. 2016M602326).

References

376 Atkins, C., Liu, Q., Minthorn, E., Zhang, S.Y., Figueroa, D.J., Moss, K., 2013. Characterization
377 of a novel perk kinase inhibitor with antitumor and antiangiogenic activity. Cancer Res. 73,
378 1993-2002.
379 Axten, J.M., Romeril, S.P., Shu, A., Ralph, J., Medina, J.R., Feng, Y., Mencken, T., 2013.
380 Discovery of GSK2656157: an optimized PERK inhibitor selected for preclinical
381 development. ACS Med. Chem. Lett. 4, 964.
382 Basseri, S., Austin, R.C., 2011. Endoplasmic reticulum stress and lipid metabolism: mechanisms
383 and therapeutic potential. Biochem. Res. Int. 2012, 1-13.
384 Basu, D., Manjur, J., Jin, W., 2011. Determination of lipoprotein lipase activity using a novel
385 fluorescent lipase assay. J. Lipid Res. 52, 826-832.
386 Beraldo, F.H., Almeida, F.M., da Silva, A.M., Garcia, C.R.S., 2005. Cyclic AMP andcalcium
387 interplay as second messengers in melatonin-dependent regulation of *Plasmodium*
388 *falciparum* cell cycle. J. Cell Biol. 170, 551-557.
389 Biwer, L., Isakson, B.E. 2016. Endoplasmic reticulum mediated signaling in cellular
390 microdomains. Acta Physiol. doi: 10.1111/apha.12675.
391 Bobrovnikova-Marjon, E., Hatzivassiliou, G., Grigoriadou, C., Romero, M., Cavener, D.R.,
392 Thompson, C.B., Diehl, J.A., 2008. PERK-dependent regulation of lipogenesis during mouse
393 mammary gland development and adipocyte differentiation. Proc Natl Acad Sci U. S. A.
394 105, 16314-16319.
395 Bozaykut, P., Sahin, A., Karademir, B., Ozer, N.K., 2016. Endoplasmic reticulum stress related
396 molecular mechanisms in nonalcoholic steatohepatitis. Mech. Ageing Dev. 157, 17-29.
397 Brasaemle D.L., Wolins N.E., 2012. Packaging of fat: an evolving model of lipid droplet
398 assembly and expansion. J Biol Chem. 278, 2273-2279.

399 Chijiwa, T., Mishima, A., Hagiwara, M., Sano, M., Hayashi, K., Inoue, T., 1990. Inhibition of
400 forskolin-induced neurite outgrowth and protein phosphorylation by a newly synthesized selective
401 inhibitor of cyclic AMP-dependent protein kinase,
402 n-[2-(p-bromocinnamylamino)ethyl]-5-isoquinolinesulfonamide (h-89), of pc12d pheochromocytoma
403 c. J. Biol. Chem. 265, 5267-72.
404 Deng, J., Liu, S., Zou, L., Xu, C., Geng, B., Xu, G., 2012. Lipolysis response to endoplasmic
405 reticulum stress in adipose cells. J. Biol. Chem. 287, 6240-6249.
406 Erbay, E., Babaev, V.R., Mayers, J.R., Makowski, L., Charles, K.N., Snitow, M.E., Hotamisligil,
407 G.S., 2009. Reducing endoplasmic reticulum stress through a macrophage lipid chaperone
408 alleviates atherosclerosis. Nat. Med. (NY, U. S.) 15, 1383-1391.
409 Erickson, B., Selvan, S.P., Ko, K.W., Kelly, K., Quiroga, A.D., Li, L., Nelsona, R., King-Jonesd,
410 K., Jacobs, R.L., Lehner, R. 2013. Endoplasmic reticulum-localized hepatic lipase decreases
411 triacylglycerol storage and VLDL secretion. Biochim. Biophys. Acta, Mol. Cell Biol. Lipids
412 1831, 1113-1123.
413 Ferreiro, E., Oliveira, C.R., Pereira, C., 2004. Involvement of endoplasmic reticulum Ca^{2+}
414 release through ryanodine and inositol 1, 4, 5- triphosphate receptors in the neurotoxic effects
415 induced by the amyloid- β peptide. J. Neurosci. Res. 76, 872-880.
416 Frayn, K. N., Langin, D., Holm, C., Belfrage, P., 1993. Hormone-sensitive lipase: quantitation of
417 enzyme activity and mrna level in small biopsies of human adipose tissue. Clin. Chim. Acta
418 216, 183-189.
419 Fredrikson, G., Tornqvist, H., Belfrage, P. 1986. Hormone-sensitive lipase and
420 monoacylglycerol lipase are both required for complete degradation of adipocyte
421 triacylglycerol. Biochim. Biophys. Acta 876, 288-293.
422 Gazarini, M.L., Thomas, A.P., Pozzan, T., Garcia, C.R., 2003. Calcium signaling in a low

calcium environment: how the intracellular malaria parasite solves the problem. J. Cell Biol. 161, 103-110.

Gerasimenko, J.V., Lur, G., Ferdek, P., Sherwood, M.W., Ebisui, E., Tepikin, A.V., Gerasimenko, O.V., 2011. Calmodulin protects against alcohol-induced pancreatic trypsinogen activation elicited via Ca^{2+} release through IP3 receptors. Proc. Natl. Acad. Sci. U. S. A. 108, 5873-5878.

Gentile, C.L., Frye, M., Pagliassotti, M.J., 2011. Endoplasmic reticulum stress and the unfolded protein response in nonalcoholic fatty liver disease. Antioxid. Redox Signaling 15, 505-521.

Gu, N., Guo, Q., Mao, K., Hu, H., Jin, S., Zhou, Y., 2015. Palmitate increases musclin gene expression through activation of perk signaling pathway in c2c12 myotubes. Biochem. Biophys. Res. Commun. 467, 521-526.

Han, J., Kaufman, R.J., 2016. The role of ER stress in lipid metabolism and lipotoxicity. J. Lipid Res. Doi: 10.1194/jlr.R067595.

Huang, C., Luo, Z., Hogstrand, C., Chen, F., Shi, X., Chen, Q. L., Song, Y.F., Pan, Y.X., 2015. Effect and mechanism of waterborne prolonged Zn exposure influencing hepatic lipid metabolism in javelin goby *Synechogobius hasta*. J. Appl. Toxicol. Doi: 10.1002/jat.3261.

Hogstrand C., 2012. Zinc. In Homeostasis and Toxicology of Essential Metals, Wood CM, Farrell AP, Brauner CJ (eds). Academic Press: London; 136-200.

Jia, X.E., Ma, K., Xu, T., Gao, L., Wu, S., Fu, C., 2015. Mutation of kri1l causes definitive hematopoiesis failure via perk-dependent excessive autophagy induction. Cell Res. 25, 946-962.

Kim, S. J., Tang, T., Abbott, M., Viscarra, J.A., Wang, Y., Sul, H.S., 2016. Ampk phosphorylates desnutrin/atgl and hsl to regulate lipolysis and fatty acid oxidation within

adipose tissue. Mol. Cell. Biol. MCB-00244.

Lafontan, M., Langin, D., 2009. Lipolysis and lipid mobilization in human adipose tissue. Prog. Lipid Res. 48, 275-297.

Lakshmanan, A.P., Harima, M., Suzuki, K., Soetikno, V., Nagata, M., Nakamura, T., Watanabe, K., 2013. The hyperglycemia stimulated myocardial endoplasmic reticulum (ER) stress contributes to diabetic cardiomyopathy in the transgenic non-obese type 2 diabetic rats: a differential role of unfolded protein response (UPR) signaling proteins. Int J Biochem Cell Biol 45, 438-447.

Lamming, D.W., Sabatini, D.M. 2013. A central role for mTOR in lipid homeostasis. Cell Metab. 18, 465-469.

Larsson, S., Jones, H.A., Göransson, O., Degerman, E., Holm, C., 2016. Parathyroid hormone induces adipocyte lipolysis via pka-mediated phosphorylation of hormone-sensitive lipase. Cell. Signalling, 28, 204-213.

Lee, A.H., Glimcher, L.H., 2009. Intersection of the unfolded protein response and hepatic lipid metabolism. Cell Mol. Life Sci. 66, 2835-2850.

Liu, F., Inageda, K., Nishitai, G., Matsuoka, M., 2006. Cadmium induces the expression of Grp78, an endoplasmic reticulum molecular chaperone, in LLC-PK1 renal epithelial cells. Environ. Health Perspect.114, 859-864.

Londos, C., Brasaemle, D.L., Schultz, C. J., Adler-Wailes, D.C., Levin, D.M., Kimmel, A.R., Rondinone, C.M., 1999. On the control of lipolysis in adipocytes. Ann. N. Y. Acad. Sci. 892, 155-168.

McNulty, T.J., Taylor, C.W., 1999. Extracellular heavy-metal ions stimulate Ca^{2+} mobilization in hepatocytes. Biochem. J. 339, 555-561.

Michalak, M., Robert Parker, J.M., Opas, M., 2002. Ca^{2+} signaling and calcium binding chaperones of the endoplasmic reticulum. Cell Calcium 32, 269-278.

Miyake, M., Nomura, A., Ogura, A., Takehana, K., Kitahara, Y., Takahara, K., Kurahashi, K., 2016. Skeletal muscle–specific eukaryotic translation initiation factor 2α phosphorylation controls amino acid metabolism and fibroblast growth factor 21–mediated non–cell-autonomous energy metabolism. FASEB J. 30, 798-812.

Newton, C.L., Whay, A.M., Mcardle, C.A., Zhang, M., van Koppen, C. J., Van, d. L.R., 2011. Rescue of expression and signaling of human luteinizing hormone g protein-coupled receptor mutants with an allosterically binding small-molecule agonist. Proc. Natl. Acad. Sci. U. S. A. 108, 7172-7176.

Oyadomari, S., Harding, H.P., Zhang, Y., Oyadomari, M., Ron, D., 2008. Dephosphorylation of translation initiation factor 2alpha enhances glucose tolerance and attenuates hepatosteatosis in mice. Cell Metab. 7, 520-532.

Plee-Gautier, E., Grober, J., Duplus, E., Langin, D., Forest, C. 1996. Inhibition of hormone-sensitive lipase gene expression by cAMP and phorbol esters in 3T3-F442A and BFC-1 adipocytes. Biochem. J. 318, 1057-1063.

Qian, Y., Tiffany-Castiglioni, E., 2003. Lead-induced endoplasmic reticulum (ER) stress responses in the nervous system. Neurochem. Res. 28, 153-162.

Ranasinghe, P., Wathurapatha, W.S., Ishara, M.H., Jayawardana, R., Galappatthy, P., Katulanda, P., 2015. Effects of zinc supplementation on serum lipids: a systematic review and meta-analysis. Nutr. Metab. 12, 1-16.

Ren, J., Chen, Z., Zhang, W., Li, L., Sun, R., Deng, C., Fei, Z., Sheng, Z., Wang, L., Sun, X., Wang, Z., 2011. Increased fat mass and insulin resistance in mice lacking pancreatic

492 lipase-related protein 1. J. Nutr. Biochem. 22, 691-698.
493 Reynisdottir, S., Dauzats, M., Thörne, A., Langin, D., 1997. Comparison of hormone-sensitive
494 lipase activity in visceral and subcutaneous human adipose tissue. J. Clin. Endocrinol. Metab.
495 82, 4162-6.
496 Ron, D., Walter, P., 2007. Signal integration in the endoplasmic reticulum unfolded protein
497 response. Nat. Rev. Mol. Cell Biol. 8, 519-529.
498 Song, Y.F., Luo, Z., Chen, Q.L., Liu, X., Liu, C.X., Zheng, J.L., 2013. Protective effects of
499 calcium pre-exposure against waterborne cadmium toxicity in *Synechogobius hasta*. Arch.
500 Environ. Contam. Toxicol. 65, 105-121.
501 Song, Y.F., Luo, Z., Pan, Y.X., Liu, X., Huang, C., Chen, Q.L., 2014. Effects of copper and
502 cadmium on lipogenic metabolism and metal element composition in the javelin goby
503 (*Synechogobius hasta*) after single and combined exposure. Arch. Environ. Contam. Toxicol.
504 67, 167-180.
505 Song, Y. F., Huang, C., Shi, X., Pan, Y. X., Liu, X., Luo, Z. 2016a. Endoplasmic reticulum stress
506 and dysregulation of calcium homeostasis mediate Cu-induced alteration in hepatic lipid
507 metabolism of javelin goby *Synechogobius hasta*. Aquat. Toxicol. 175, 20-29.
508 Song, Y.F., Luo, Z., Zhang, L.H., Hogstrand, C., Pan, Y.X., 2016b. Endoplasmic reticulum stress
509 and disturbed calcium homeostasis are involved in copper-induced alteration in hepatic lipid
510 metabolism in yellow catfish *Pelteobagrus fulvidraco*. Chemosphere 144, 2443-2453.
511 Song, Y.F., Wu, K., Tan, X.Y., Zhang, L.H., Zhuo, M.Q., Pan, Y.X., Chen, Q.L., 2015. Effects
512 of recombinant human leptin administration on hepatic lipid metabolism in yellow catfish
513 *Pelteobagrus fulvidraco*: *In vivo* and *in vitro* studies. Gen. Comp. Endocrinol. 212, 92-99.
514 Tang, C. H. A., Ranatunga, S., Kriss, C. L., Cubitt, C. L., Tao, J., Pinilla-Ibarz, J. A., Hu, C. C.

A., 2014. Inhibition of ER stress–associated IRE-1/XBP-1 pathway reduces leukemic cell survival. J. Clin. Invest., 124, 2585-2598.

Taylor C. W., Laude A. J. 2002. IP3 receptors and their regulation by calmodulin and cytosolic Ca^{2+}. Cell Calcium 32, 321-334.

Tufanli, O., Akillilar, P.T., Acosta-Alvear, D., Kocaturk, B., Onat, U.I., Hamid, S. M., Erbay, E. 2017. Targeting IRE1 with small molecules counteracts progression of atherosclerosis. Proc. Natl. Acad. Sci. U. S. A. 114, E1395-E1404.

Volmer, R., Ron, D. 2015. Lipid-dependent regulation of the unfolded protein response. Curr. Opin. Cell Biol., 33, 67-73.

Wang, S., Kaufman, R.J., 2012. The impact of the unfolded protein response on human disease. J. Cell Biol. 197, 857-867.

Xu, C., Bailly-Maitre, B., Reed, J.C., 2005. Endoplasmic reticulum stress: cell life and death decisions. J. Clin. Invest. 115, 2656-2664.

Yusta, B., Baggio, L. L., Estall, J. L., Koehler, J. A., Holland, D.P., Li, H. 2006. Glp-1 receptor activation improves β cell function and survival following induction of endoplasmic reticulum stress. Cell Metab. 4, 391-406.

Zechner, R., Zimmermann, R., Eichmann, T. O., Kohlwein, S. D., Haemmerle, G., Lass, A., Madeo, F., 2012. FAT SIGNALS-lipases and lipolysis in lipid metabolism and signaling. Cell Metab. 15, 279-291.

Zhang, C., Chen, X., Zhu, R.M., Zhang, Y., Yu, T., Wang, H., Zhao, H., Zhao, M., Jia, Y.L., Chen, Y.H., Meng, X.H., Wei, W., Xu, D.X., 2012. Endoplasmic reticulum stress is involved in hepatic SREBP-1c activation and lipid accumulation in fructose-fed mice. Toxicol. Lett. 212, 229-240.

538 Zheng, D.L., Kille, P., Feeney, G.P., Cunningham, P., Handy, R.D., & Hogstrand, C. 2010.
539 Dynamic transcriptomic profiles of zebrafish gills in response to zinc supplementation. BMC
540 Genomics 11, 1-17.
541 Zheng, J.L., Luo, Z., Liu, C.X., Chen, Q.L., Tan, X.Y., Zhu, Q.L., Gong, Y.. 2013. Differential
542 effects of acute and chronic zinc (Zn) exposure on hepatic lipid deposition and metabolism in
543 yellow catfish *Pelteobagrus fulvidraco*. Aquat. Toxicol. 132-133, 173-181.
544 Zheng, J. L., Luo, Z., Zhu, Q. L., Hu, W., Zhuo, M. Q., Pan, Y. X., Song, Y.F., Chen, Q. L.,
545 2015. Different effect of dietborne and waterborne Zn exposure on lipid deposition and
546 metabolism in juvenile yellow catfish *Pelteobagrus fulvidraco*. Aquat. Toxicol. 159, 90-98.
547 Zhuo, M.Q., Luo, Z., Wu, K., Zhu, Q.L., Zheng, J.L., Zhang, L.H., Chen, Q.L., 2014. Regulation
548 of insulin on lipid metabolism in freshly isolated hepatocytes from yellow catfish
549 (*Pelteobagrus fulvidraco*). Comp. Biochem. Physiol. B. 177, 21-28.
550
551
552

Figure captions

FIGURE. 1. Chronic Zn exposure caused ER stress and UPR in liver of *P. fulvidraco in vivo*. (A) Liver ultrastructure (TEM, original magnification ×10000, bars 1 μm) of *P. fulvidraco* exposed to waterborne Zn at concentrations 0 mg/l, 0.25 mg/l and 0.5 mg/l for 28 days and 56 days. Abbreviation: mitochondria (m); hepatocyte nucleus (nu); endoplasmic reticulum (er); swelling and vesiculation of mitochondria (sw); swelling of endoplasmic reticulum (ser). Liver cells of fish in the control, showing the typical appearance of mitochondria with clear cristae and ER with flat, branched cisternal spaces delimited by ribosome-bearing membranes. Hepatocytes in Zn groups showed the swelling of mitochondria and ER, and these alterations increased with increasing Zn levels. (B and C) Zn exposure up-regulated the expression of genes involved in ER stress and UPR *in vivo*. Values are mean ± SEM (n = 3 replicate tanks, three fish were sampled for each tank). mRNA expression values were normalized to β-actin and TUBA expressed as a ratio of the control on day 28 (control = 1). Different letters indicate significant differences among groups for the same exposure time. Asterisks indicate significant differences between day 28 and day 56 for the same Zn concentrations ($P < 0.05$).

FIGURE. 2. Chronic Zn exposure up-regulated lipolysis in liver of *P. fulvidraco in vivo*. (A and B) Chronic Zn exposure up-regulated the expression of genes involved in UPR and cAMP/PKA pathway *in vivo*. mRNA expression values were normalized to β-actin and TUBA expressed as a ratio of the control on day 28 (control = 1). (C, D and E) Effects of chronic Zn exposure on the levels of cAMP and PKA (C), the activity of lipase,

HSL and ATGL (D), and the contents of TG and glycerol (E), in liver of *P. fulvidraco in vivo*. Values are mean ± SEM (n = 3 replicate tanks, three fish were sampled for each tank). mRNA expression values were normalized to β-actin and TUBA expressed as a ratio of the control on day 28 (control = 1). Different letters indicate significant differences among groups for the same exposure time. Asterisks indicate significant differences between day 28 and day 56 for the same Zn concentrations ($P < 0.05$).

FIGURE. 3. Zn treatment causes disturbed Ca^{2+} homeostasis *in vitro*. (A) Cells were stimulated with (30 μM) at the designated times (60s) and fluorescence ratio (*F/F0*) intensity was plotted as a function of time. (B and C) Cells were treated with 30 μM Zn in the presence of 30 μM dantrolene or 50 μM 2-APB. (D) Summary of Zn-induced increase in fluorescence ratio. Each column represents the mean ± SEM. Data summarize three independent experiments. Different letters indicated significant differences among groups (Control = DMSO treatment, data not shown) ($P< 0.05$). The experiments were repeated three times with similar results and a representative experiment is shown. Zn was applied as indicated by upward arrows. Representative fluorescence measurements are shown at different designated time points (10s, 120s and 240s).

FIGURE. 4. Differential effects of PERK-eIF2α and IRE1α-XBP1 on Zn-induced hepatic lipolysis *in vitro*. (A and B) STF-083010 alleviates the activation of IRE1α-XBP1 pathway induced by Zn, and influences the expression of genes involved in lipolysis. The genes' expression involved in PERK-eIF2α pathway are denoted by a dotted lines box. mRNA expression values were normalized to β-actin and TUBA expressed as a ratio of

the control (control = 1). (C, D and E) Effects of STF-083010 on the levels of cAMP and PKA (C), the activity of lipase, HSL and ATGL (D), and the contents of TG and glycerol (E) in primary hepatocytes from *P. fulvidraco in vitro*. Differential effects of GSK2656157 and STF-083010 on the Zn-induced hepatic lipolysis denoted by a solid lines box. Values are mean ± SEM (n= 3 independent biological experiments). Different letters indicated significant differences among groups. Asterisks indicate significant differences between Zn groups and Zn + STF-083010 groups, and also between Zn + GSK2656157 groups and Zn + STF-083010 groups ($P < 0.05$).

FIGURE. 5. ER stress and UPR up-regulated lipolysis via the activation of cAMP/PKA signaling pathway *in vitro*. (A and B) H 89 alleviated the Zn-induced activation of cAMP/PKA pathway, and influenced the expression of genes involved in ER stress and lipolysis. The genes' expression involved in cAMP/PKA pathway are denoted by a dotted lines box. mRNA expression values were normalized to β-actin and TUBA expressed as a ratio of the control (control = 1). (C, D and E) Effects of H 89 on the levels of cAMP and PKA (C), the activity of lipase, HSL and ATGL (D), and the contents of TG and glycerol (E) in primary hepatocytes from *P. fulvidraco in vitro*. Values are mean ± SEM (n= 3 independent biological experiments). Different letters indicated significant differences among groups. Asterisks indicate significant differences between Zn groups and Zn + H 89 groups ($P < 0.05$).

Fig. 1

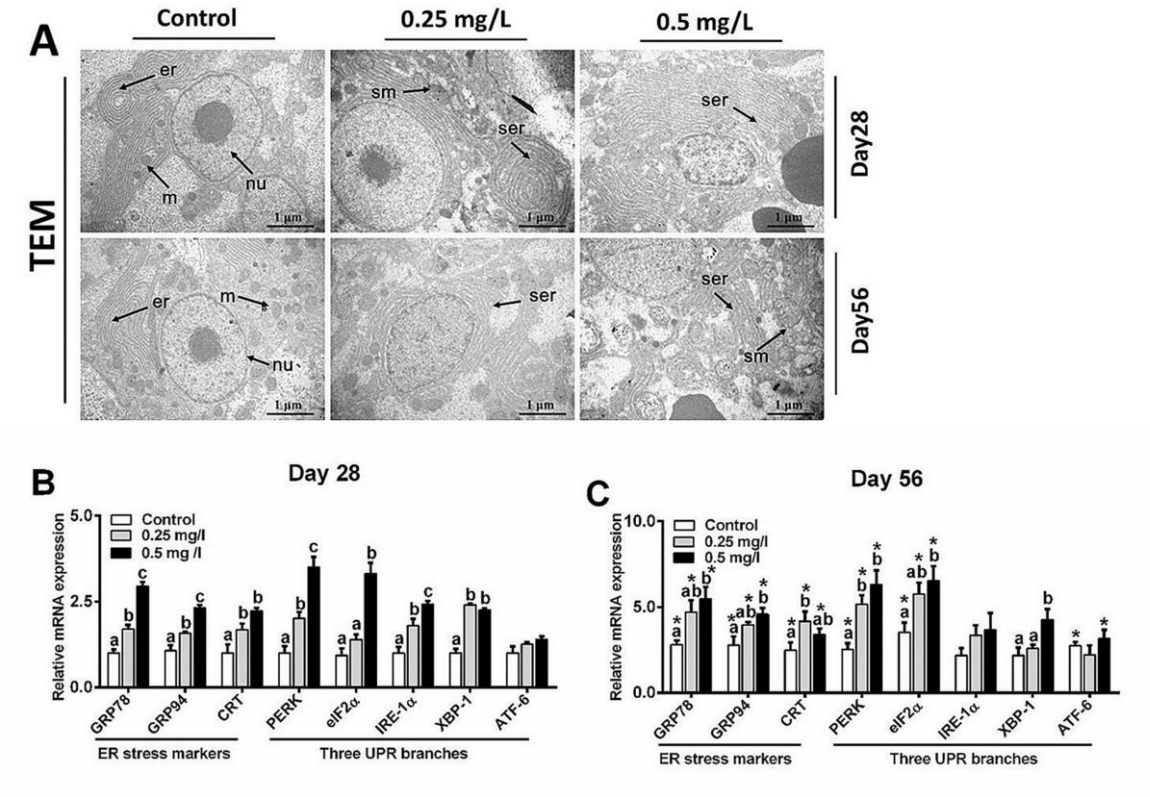
A
Control
0.25 mg/L
0.5 mg/L
TEM
Day28
Day56
er
m
nu
sm
ser
1 μm
B
Day 28
C
Day 56
Control
0.25 mg/l
0.5 mg /l
Relative mRNA expression
GRP78
GRP94
CRT
PERK
eIF2α
IRE-1α
XBP-1
ATF-6
ER stress markers
Three UPR branches

Fig. 2

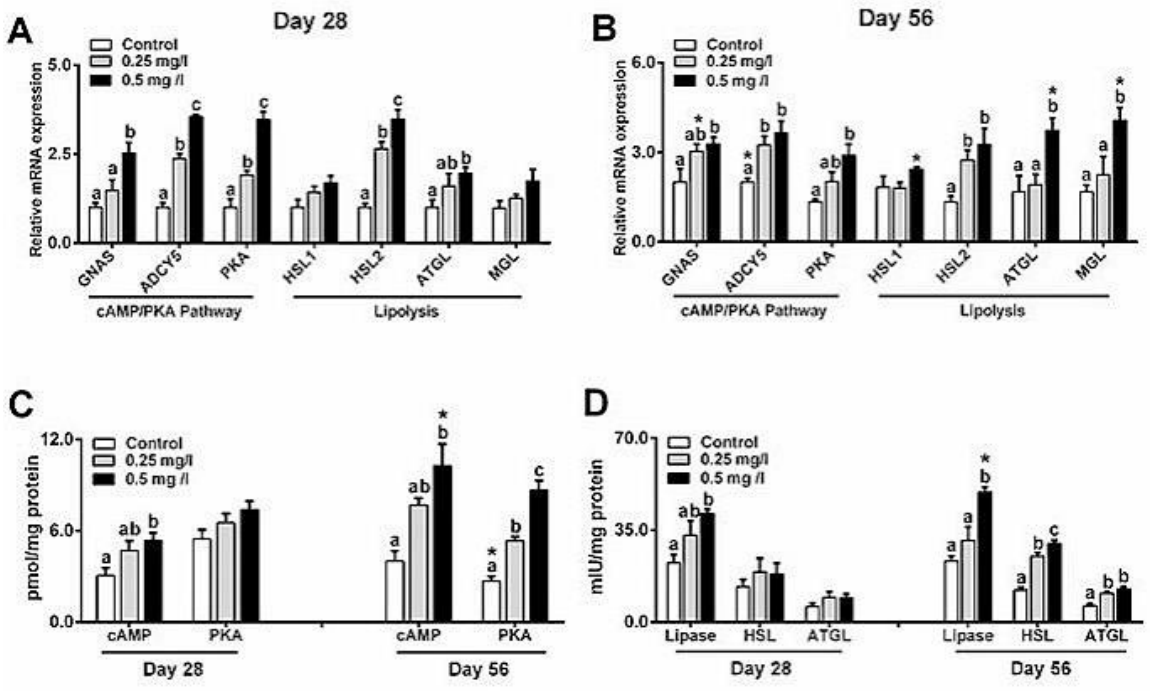
A
Day 28
Control
0.25 mg/l
0.5 mg /l
Relative mRNA expression
5.0
2.5
0.0
GNAS
ADCY5
PKA
HSL1
HSL2
ATGL
MGL
cAMP/PKA Pathway
Lipolysis
B
Day 56
Control
0.25 mg/l
0.5 mg /l
Relative mRNA expression
6.0
3.0
0.0
GNAS
ADCY5
PKA
HSL1
HSL2
ATGL
MGL
cAMP/PKA Pathway
Lipolysis
C
Control
0.25 mg/l
0.5 mg /l
pmol/mg protein
12.0
6.0
0.0
cAMP
PKA
cAMP
PKA
Day 28
Day 56
D
Control
0.25 mg/l
0.5 mg /l
mIU/mg protein
70.0
35.0
0.0
Lipase
HSL
ATGL
Lipase
HSL
ATGL
Day 28
Day 56

Fig. 3

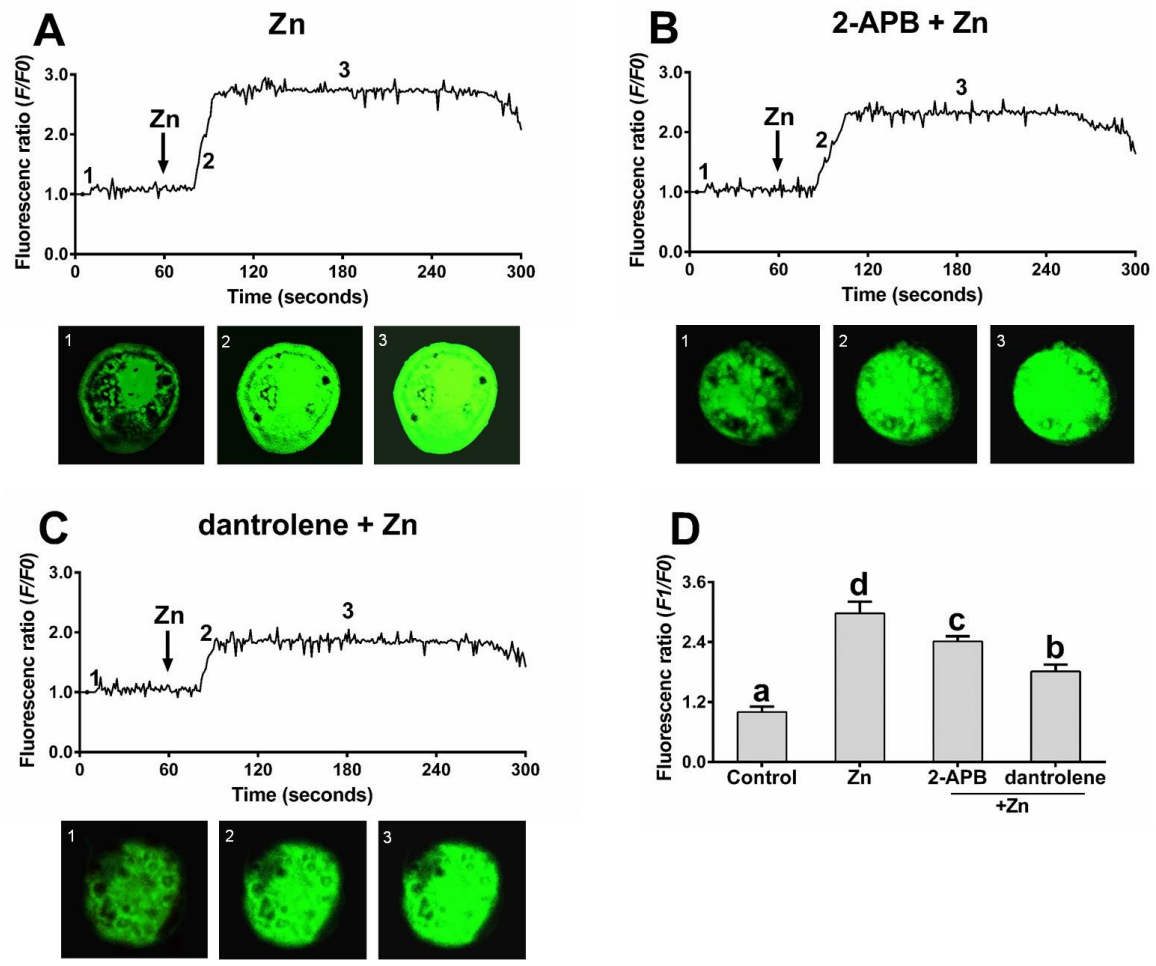
A
Zn
Fluorescenc ratio (F/F0)
Time (seconds)
B
2-APB + Zn
C
dantrolene + Zn
D
Fluorescenc ratio (F1/F0)
Control
Zn
2-APB
dantrolene
+Zn

Fig. 4

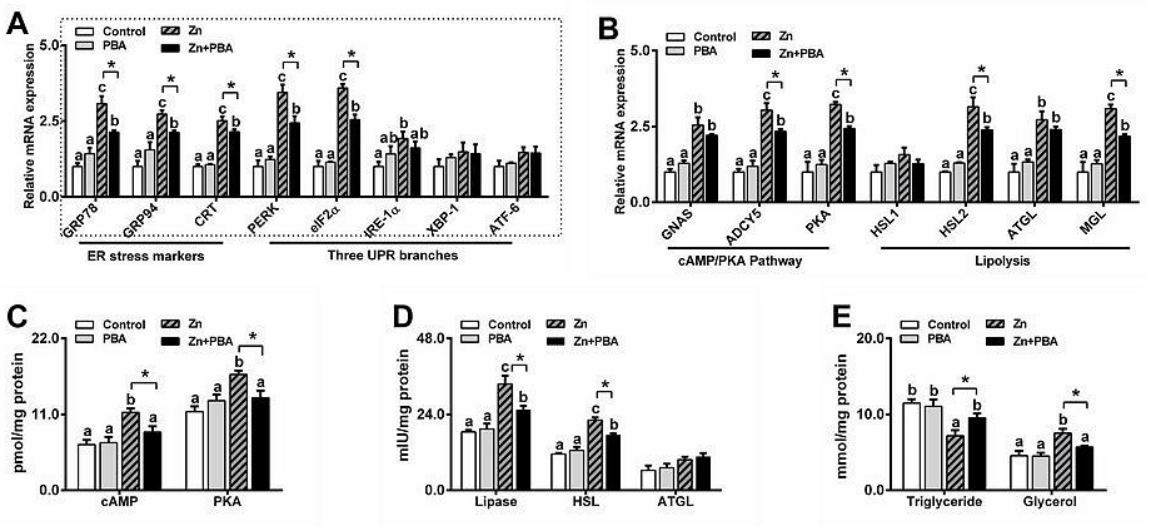
A
Control
PBA
Zn
Zn+PBA
Relative mRNA expression
5.0
2.5
0.0
GRP78
GRP94
CRT
PERK
eIF2α
IRE-1α
XBP-1
ATF-6
ER stress markers
Three UPR branches
B
Control
PBA
Zn
Zn+PBA
Relative mRNA expression
5.0
2.5
0.0
GNAS
ADCY5
PKA
HSL1
HSL2
ATGL
MGL
cAMP/PKA Pathway
Lipolysis
C
Control
PBA
Zn
Zn+PBA
pmol/mg protein
22.0
11.0
0.0
cAMP
PKA
D
Control
PBA
Zn
Zn+PBA
mIU/mg protein
48.0
24.0
0.0
Lipase
HSL
ATGL
E
Control
PBA
Zn
Zn+PBA
mmol/mg protein
20.0
10.0
0.0
Triglyceride
Glycerol

Fig. 5

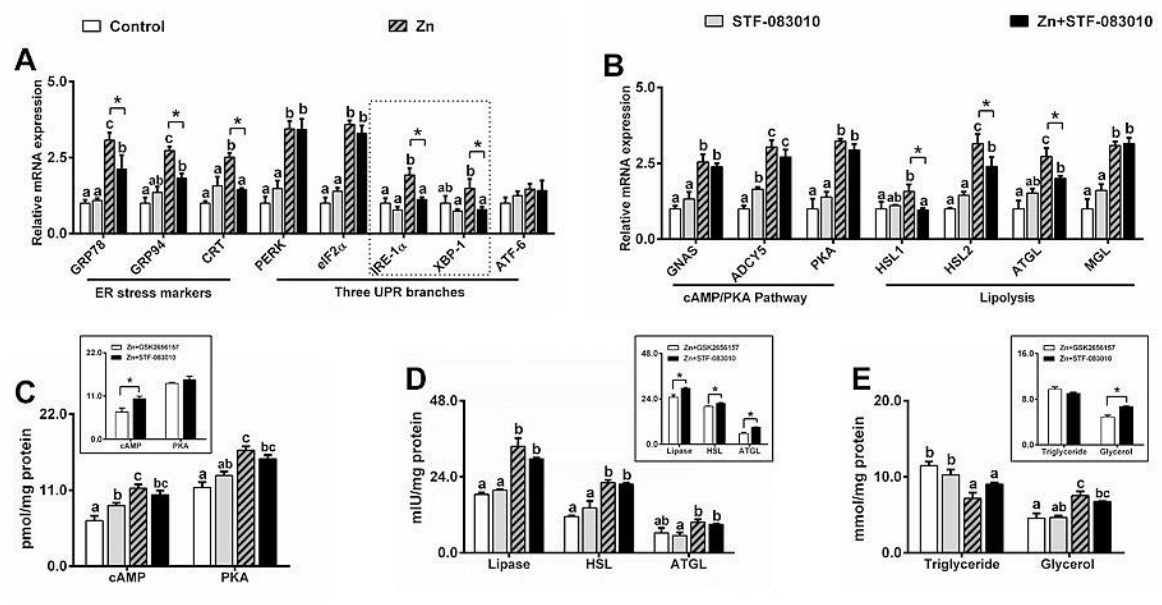
A
Control
Zn
Relative mRNA expression
GRP78
GRP94
CRT
PERK
eIF2α
IRE-1α
XBP-1
ATF-6
ER stress markers
Three UPR branches
B
STF-083010
Zn+STF-083010
Relative mRNA expression
GNAS
ADCY5
PKA
HSL1
HSL2
ATGL
MGL
cAMP/PKA Pathway
Lipolysis
C
pmol/mg protein
cAMP
PKA
D
mIU/mg protein
Lipase
HSL
ATGL
E
mmol/mg protein
Triglyceride
Glycerol

Fig. 6

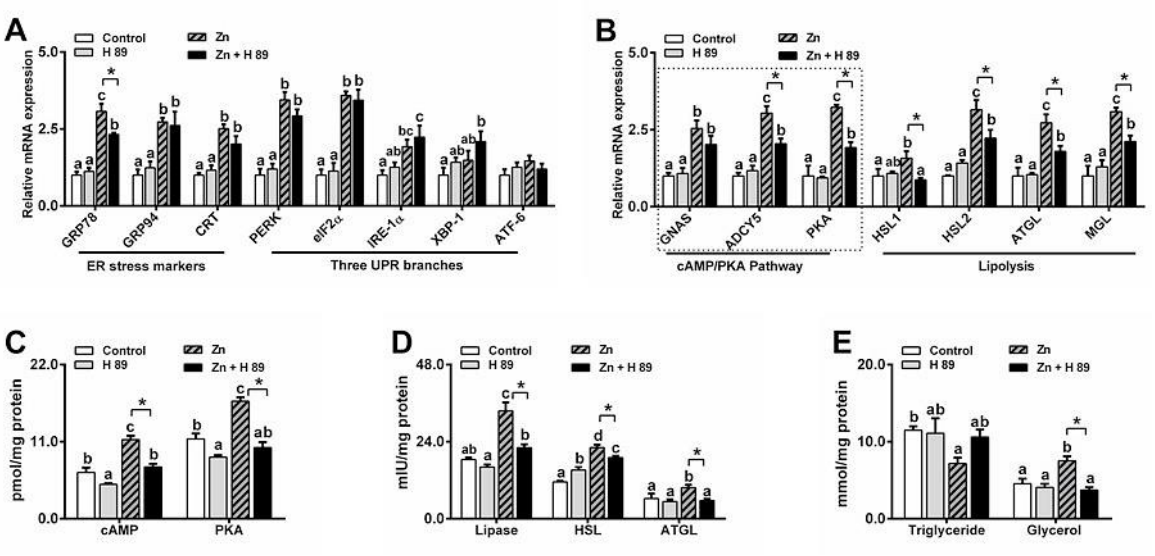
A
Control
H 89
Zn
Zn + H 89
Relative mRNA expression
5.0
2.5
0.0
GRP78
GRP94
CRT
PERK
eIF2α
IRE-1α
XBP-1
ATF-6
ER stress markers
Three UPR branches
B
GNAS
ADCY5
PKA
HSL1
HSL2
ATGL
MGL
cAMP/PKA Pathway
Lipolysis
C
pmol/mg protein
22.0
11.0
cAMP
PKA
D
mIU/mg protein
48.0
24.0
Lipase
HSL
ATGL
E
mmol/mg protein
20.0
10.0
Triglyceride
Glycerol